Electronic structure at carbon nanotube tips studied by photoemission spectroscopy

S. Suzuki,* Y. Watanabe, T. Kiyokura,† K. G. Nath, and T. Ogino
NTT Basic Research Laboratories, Atsugi, Kanagawa, 243-0198 Japan

S. Heun
Sincrotrone Trieste, Basovizza, 34012 Trieste, Italy

W. Zhu
Bell Laboratories, Lucent Technologies, Murray Hill, New Jersey 07974

C. Bower‡ and O. Zhou
Department of Physics and Astronomy and Curriculum in Applied and Materials Science, University of North Carolina, Chapel Hill, North Carolina 27599

(Received 26 December 2000; published 8 June 2001)

The valence band and C 1*s* photoemission spectra were measured from the tips and the sidewalls of multiwalled carbon nantoubes grown on Si substrates. The results show an overall spectral shift to the higher-binding-energy side, a larger density of states at the Fermi level, and a lower work function at the tips. These results can be explained by assuming that the Fermi level is slightly shifted upward and located inside the conduction band at the tips. We suggest that the electronic structure at the tips is considerably affected by defects.

DOI: 10.1103/PhysRevB.63.245418 PACS number(s): 61.48.+c

I. INTRODUCTION

Since the discovery of carbon nanotubes, their electronic structure has attracted much attention because of their nanometer-scale highly one-dimensional structure. More interestingly, a specific electronic structure is expected at the tips of nanotubes, where the graphene cylinders are believed to be closed by insertion of the five-member rings in the graphene network. The investigation of the electronic properties of nanotube tips is also important for understanding the electron field-emission properties of nanotubes.[1–3]

The local electronic structure of carbon nanotubes has been extensively studied using scanning tunneling spectroscopy (STS). As predicted by theory,[4] it has been confirmed that nanotubes have a wide variety of electronic structures and become metallic or semiconducting, depending on the helicity.[5] Furthermore, the local density of states at nanotube tips has also been reported. Sharp resonances in the vicinity of the Fermi level have been observed at the tips of both a multiwalled nanotube[6] (MWNT) and a single-walled nanotube[7] (SWNT). The STS peaks observed in the band gaps were basically interpreted as the localized electronic states induced by the five-member rings. The energy positions of the peaks in the band gaps were found to oscillate along the tube axes near the tube tips.[8]

Although STS is a unique analytical technique for investigating the local density of states of a nanotube, one of its disadvantages is that the energy range of the spectra is strictly limited near the Fermi level (typically ± 1 eV). Thus, the overall band structure cannot be probed. In contrast, photoemission spectroscopy can provide information about the electronic structure over a wide energy range including core levels. Moreover, it can directly determine the work function, which is crucial for understanding the electron field-emission properties, without employing any uncertain parameters. Therefore, it is worthwhile to investigate the electronic structure of carbon nanotubes using photoemission spectroscopy.

We measured the valence band and C 1*s* photoemission spectra and work functions of vertically aligned and random MWNT's grown on Si substrates. The spectra from the aligned MWNT's were considered to be dominated by photoemission from the tips. We found that the aligned MWNT's showed a larger density of states at the Fermi level and a smaller work function. A slight energy shift of the overall electronic states to the higher-binding-energy side was also observed. The results will be discussed in terms of the electronic structural differences between the tips and sidewalls of the carbon nanotubes. We suggest that defects in the MWNT's play an important role in explaining the experimental results.

II. EXPERIMENT

The MWNT's aligned perpendicularly on a Si substrate were grown using the microwave plasma-enhanced chemical vapor deposition (MPB-CVD) method. A typical scanning electron microscope (SEM) image of the MPB-CVD-grown aligned MWNT's is shown in Fig. 1(a). The diameter and length of the MWNT's were about 30 nm and 10 μm, respectively. Details of the synthesis are described elsewhere.[9] The random MWNT's, whose typical diameter was 20–50 nm, were also grown on a Si substrate using the thermal CVD technique [Fig. 1(b)].

Photoemission measurements were carried out at beam line BL-1*C*, Photon Factory, High Energy Accelerator Research Institute, Japan, using an angle-integrated-type hemispherical electron energy analyzer. Both monochromatized

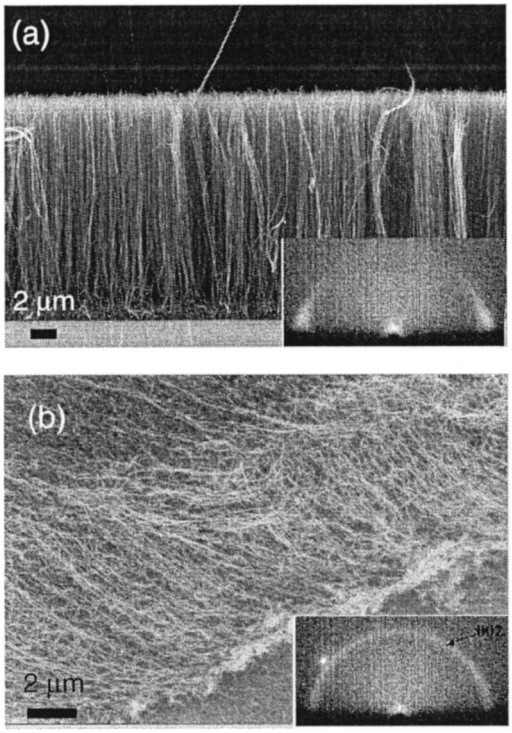

FIG. 1. SEM image of the (a) aligned MWNT's and (b) random MWNT's. The insets are (002) x-ray diffraction patterns that show that the nanotubes are (a) vertically aligned and (b) randomly oriented.

synchrotron radiation light and a He discharge lamp were used as light sources. The measurements were carried out at room temperature. The overall energy resolutions, which were mostly determined by the Fermi-Dirac distribution function, were estimated to be 0.1 eV for the valence-band spectra and 0.2 eV for the C 1*s* spectra (second-order light was used). Before the measurements, the samples were annealed at 300 °C in a vacuum to remove adsorbates on the surfaces. The base pressure of the analysis chamber was 1×10^{-9} mbar. The position of the Fermi level was calibrated by measuring the Fermi edge of an evaporated gold film.

III. RESULTS

As is well known, the excitation probability of the optical transition is proportional to $|\langle f|\mathbf{A}\cdot\mathbf{P}|i\rangle|^2$, where $|i\rangle$ and $|f\rangle$ are initial and final electronic states, **A** is the vector potential of the incident photon, and **P** is the momentum operator. Because the initial electronic states $|i\rangle$ in a nanotube are highly anisotropic, it can be expected that the photoemission spectrum from a nanotube sidewall depends on the polarization direction determined by **A**. On the other hand, the photoemission from a nanotube tip is considered to be independent of the polarization direction because it is hemispherical. Figure 2 shows the valence-band spectra of the aligned MWNT's taken at different polarization directions. In the figure, θ_i denotes the angle between the incident synchrotron radiation light and the surface normal of the sample. The photoemission take-off angles θ_e were 0° and 45° for θ_i of

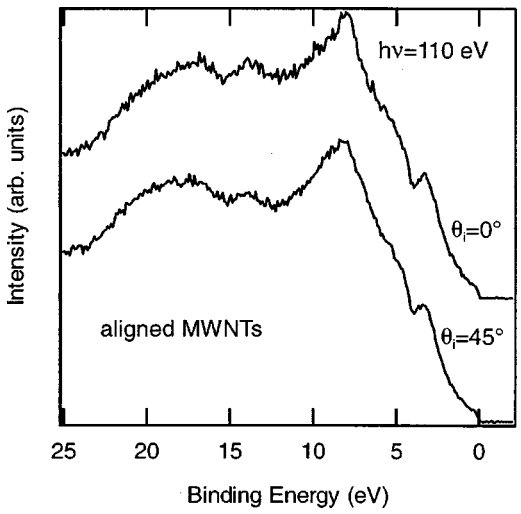

FIG. 2. Valence-band photoemission spectra of the aligned MWNT's taken at different incident angles.

45° and 0°, respectively. As shown in the figure, no distinct polarization dependence was observed in the valence-band spectra of the aligned sample, although the nanotubes were highly oriented. The slight spectral difference observed above ~15 eV may mainly be due to a difference in the signal-to-background ratios, because the spectral difference was much reduced by background subtraction, assuming Shirley-type backgrounds (not shown). This result indicates that the spectra from the aligned MWNT's were dominated by photoemission from the tube tips rather than by that from the sidewalls. This is not surprising because the nanotube caps were exposed at the sample surface as shown in Fig. 1(a) and because the photoemission technique is very surface sensitive (typical probing depth is a few nanometers). On the other hand, spectra from the random MWNT's are considered to be dominated by photoemission from sidewalls, because nanotubes are much longer than the tip radii.

Figure 3 shows the valence-band spectra of the aligned and random MWNT's taken at a photon energy of 100 eV.

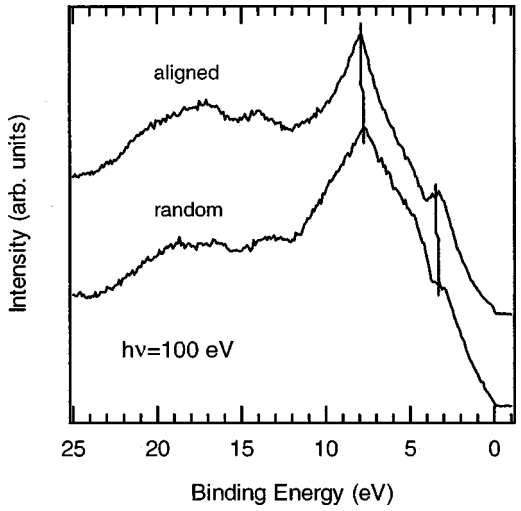

FIG. 3. Valence-band photoemission spectra of the aligned and random MWNT's.

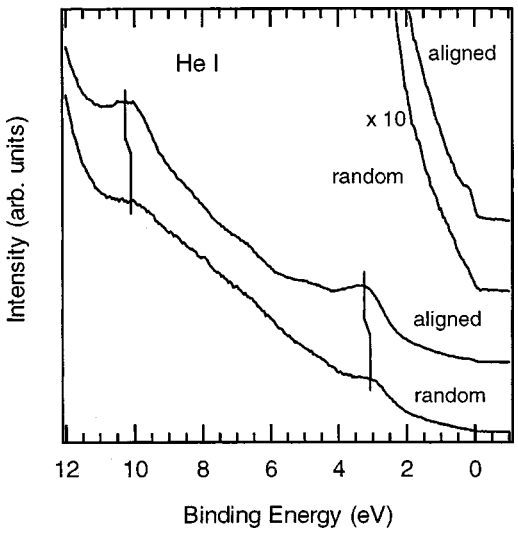

FIG. 4. Ultraviolet photoemission spectra of the aligned and random MWNT's.

Hereafter, we show the spectra obtained at the normal emission condition ($\theta_e = 0°$). We can say that the spectral intensity around the 3.5-eV peak is predominantly due to the π bands, and the 8-eV peak and higher-energy region are due to σ bands, respectively, on the basis of a previous x-ray emission spectroscopy study on graphite.[10] Although the overall spectral features are quite similar to each other and to the spectrum of unaligned MWNT's obtained in a previous study,[11] we can see that the peak positions of the unaligned MWNT's shifted to the higher-binding-energy side by about 0.2 eV. Moreover, it is obvious that the spectral intensity at the Fermi level of the aligned MWNT's is much higher than that of the random MWNT's. An energy shift similar to that of Fig. 3 was observed in the valence-band spectra taken at 21.2 eV (He *I*), as shown in Fig. 4. The peaks of the aligned MWNT's are located at higher binding energy by 0.1–0.2 eV. The larger density of states at the Fermi level of the aligned MWNT's was also observed, although it is less prominent than that in Fig. 3.

Figure 5 shows the spectra in the vicinity of the Fermi level of the aligned and random MWNT's taken at 100 eV. For reference, the spectrum of random SWNT's (tube and bundle diameters[12] of 1.4 and ~20 nm) is also shown. For the aligned MWNT's, the existence of the Fermi edge is obvious. Although some valence-band photoemission studies of unaligned MWNT's have been reported,[11,13] such clear Fermi edges (Figs. 3–5) from MWNT's have not been observed. This strongly suggests a specific electronic structure at the tips of the aligned MWNT's. A Fermi-edge-like feature is also slightly observed in the random MWNT's, although the spectral intensity at the Fermi level is apparently lower than that of the aligned MWNT's. On the other hand, the SWNT's show a very small spectral intensity at the Fermi level. Thus, we can conclude that the density of states at the Fermi level decreases in order of the aligned MWNT's, random MWNT's, and the SWNT's. Note that graphite, as well as the SWNT's, shows a very small spectral intensity at the Fermi level.[14]

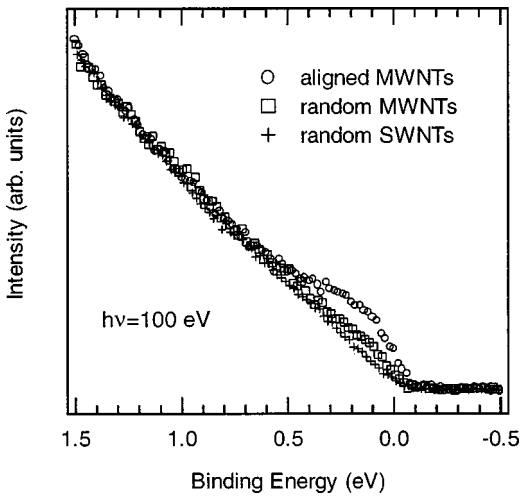

FIG. 5. Photoemission spectra in the vicinity of the Fermi level of the aligned and random MWNT's and the SWNT's.

Figure 6 shows the C 1*s* spectrum of the aligned and random MWNT's. Previously, some authors[13,15] concluded, from analyses of C 1*s* spectra obtained by conventional x-ray photoelectron spectroscopy (XPS), that multiwalled nanotubes are considerably oxidized. According to their curve-fitting analyses, the oxidized components were located at a binding energy about 1 eV above the main peak and at higher energies. However, no oxidized component is observed in Fig. 6, although the spectra were obtained at a much higher energy resolution than conventional XPS. Thus, we conclude that the surfaces of both the aligned and random MWNT's were little oxidized. Both spectra had tails at the higher-binding-energy side, which are indicative of core-hole screening by conductive electrons.[16] The spectral asymmetry of the aligned MWNT's is larger than that of the random MWNT's. This is consistent with the above observation of the larger density of states at the Fermi level in the aligned MWNT's.

As in the case of the valence-band states shown in Figs. 3

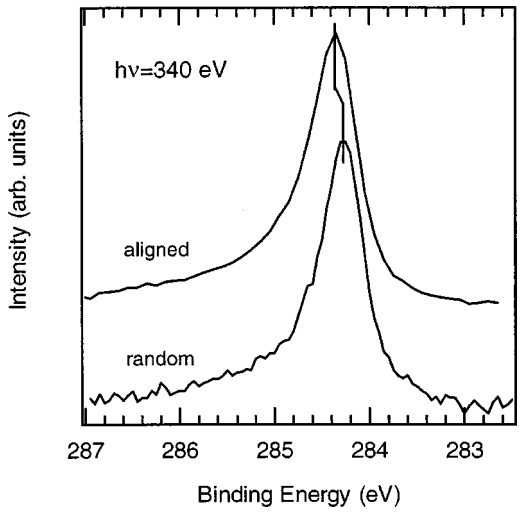

FIG. 6. C 1*s* photoemission spectra of the aligned and random MWNT's.

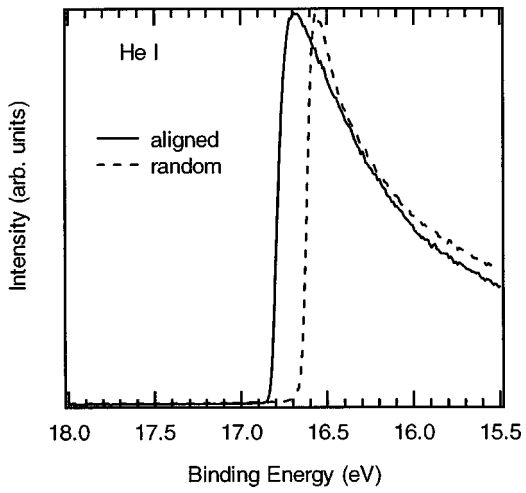

FIG. 7. Secondary-electron threshold spectra of the aligned and random MWNT's.

and 4, the peak position of the aligned MWNT's shifts toward the higher-binding-energy side by about 0.1 eV. These results indicate that the overall electronic structure, including both the valence bands and the core levels observed in the aligned MWNT's, is slightly shifted to the higher-binding-energy side.

Figure 7 shows the secondary-electron threshold spectra of the aligned and random MWNT's excited by a He discharge lamp. The work functions Φ can simply be determined from the secondary-electron threshold energy as $\Phi = h\nu - E_{\rm th}$, where $h\nu$ and $E_{\rm th}$ are the photon energy of the excitation light (21.22 eV) and the nominal binding energy of the threshold energy. The work function of the random MWNT's was determined to be about 4.6 eV. This value is close to the value for graphite obtained in our previous study[17] (4.6–4.7 eV) and in other photoemission studies[18,19] (4.6 eV). On the other hand, the work function of the aligned MWNT's was determined to be 4.4 eV, which is smaller than those of the random MWNT's and graphite. It is worth noting that this result is consistent with our previous report,[20] which showed that the threshold voltage of electron field emission of aligned MWNT's is lower than that of random MWNT's. Interestingly, the work function of the SWNT's, in contrast to the aligned MWNT's, was found to be 4.8 eV in our previous study,[17,21] which is a slightly larger value than that for graphite.

There have been a few studies on the work function of random MWNT's, using photoemission spectroscopy.[11,13] Ago *et al.*[13] reported a value of 4.3 eV (graphite: 4.4 eV). Chen *et al.*[11] also reported a slightly smaller work function for random MWNT's than that for graphite; however, their spectra (Fig. 2 of Ref. 11) give values of 5.75 eV for random MWNT's and 5.85 eV for graphite, which seem to be too large. Although the reason for the differences in the actual values is not clear, it seems that the work functions of random MWNT's and graphite are close. Here, we would like to stress that our results reveal that the work function of the tips of the aligned MWNT's is smaller than the work functions of the random MWNT's and graphite.

IV. DISCUSSION

Here, we discuss a possible interpretation of the observed results. As stated above, the spectra from the aligned MWNT's are considered to be dominated by photoemission from tube tips rather than by that from the sidewalls. Therefore, the results indicate that the binding energy of the overall electronic structure, including the core level, at the tips of the aligned MWNT's is slightly larger than that of the sidewalls of the random MWNT's. The results also indicate that the tips of the aligned MWNT's have a larger density of states at the Fermi level and a smaller work function.

The rigid shift behavior of the overall electronic structure strongly suggests that the Fermi level is shifted from the ideal position and is pinned slightly inside the conduction band at the tips of the aligned MWNT's [hereafter, in this sense, we call the Fermi-level movement the ''upward Fermi level shift,'' although the Fermi level should be uniform at any part in MWNT (see Fig. 9)]. Thus, the density of states at the Fermi level should be increased as observed in Figs. 3–5. The smaller work function observed in the aligned MWNT's can also be simply explained in terms of the upward Fermi-level shift, because this shift will reduce the energy difference between the vacuum level and the Fermi level.

As discussed above, the binding-energy shift, the large density of states, and the smaller work function observed in the aligned MWNT's can be well explained by assuming the upward Fermi-level shift at the tips. However, the origin of the Fermi-level pinning is still an open question. A Fermi-level shift caused by adsorption of gas molecules such as O_2 can be excluded because the sample was annealed just before the measurement. Moreover, a recent theoretical calculation predicted that adsorption of O_2 on a nanotube surface would cause a downward Fermi-level shift,[22] which is contrary to our experimental results. The insertion of the five-member rings in the graphene network at tips will induce a singularity of the density of states near the Fermi level.[6,7,23] However, this cannot explain the large density of states just at (not only near) the Fermi level that we observed in the aligned MWNT's. The observed spectral difference (Fig. 5) between the random MWNT's and SWNT's is not explained by effects induced by the five-member rings either, because both spectra are dominated by photoemission from the sidewalls. The electronic structure of the graphene sheets should also be modified by the curvature of the sheets. The curvature effect may explain why the work function[17,21] of SWNT's is slightly larger than that of graphite: *s* orbital mixing into the π states caused by the curvature may decrease the energy of the π states, and thus increase the work function.[24,25] According to this idea, however, the work function of the tips, where the electronic structure will be more affected by the curvature, should be larger than that of the sidewalls, and this is completely contrary to the experimental result. It is also difficult to explain, by curvature effects, why the thin SWNT's and graphite showed very small densities of states at the Fermi level, in spite of the fact that the thick aligned and random MWNT's showed Fermi-edge-like features. Furthermore, we should note that the diameter of the aligned

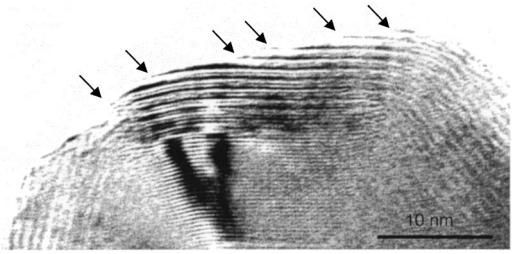

FIG. 8. TEM image of the tip of a second stage *K*-intercalated MWNT.

MWNT's was quite large, about 30 nm. Therefore, it is expected that, in this case, the electronic structure at the tips is not significantly affected by the insertion of the five-member rings or by the curvature. Thus, it seems to be difficult to explain all the experimental results on the aligned MWNT's and random MWNT's and SWNT's assuming that the nanotubes have ideal (perfectly closed packed) structures.

The Fermi level can be pinned inside the conduction band if defect states (in this paper, ''defect'' means breaks in the graphene sheets, not the five- or seven-member ring) are formed inside the conduction band and the defect density is sufficiently large. Our previous study[26] using an analytical electron microscope revealed that most MWNT's were intercalated by alkali-metal atoms deposited on the MWNT's in vacuum. A typical example of a tip of a second-stage *K*-intercalated MWNT is shown in Fig. 8. The nanotube is intercalated from the surface to a depth of about 10 nm. The intercalation indicates that the nanotube did not have a close-packed structure, but a *papier maché* structure.[27] Actually, some breaks in the graphene sheets are clearly observed in the figure (denoted by arrows). Such breaks were often observed at tips after the intercalation (although they were seldom observed before the intercalation). It is considered that the aligned and the random MWNT's measured in this study were also defective enough to be intercalated, because a spectral shift to the higher-binding-energy side and a significant increase of the density of states at the Fermi level, which are indicative of an intercalation reaction,[17,21] were observed in the valence-band photoemission spectra after Cs deposition in vacuum.[28]

If the Fermi-level pinning is caused by the defect states, the defect density should be large enough for the observed upward Fermi-level shift of 0.1–0.2 eV. We can roughly expect that the density of states in the vicinity of the Fermi level of a MWNT is about 0.02 states per electron volt per atom, by referring to a band-structure calculation for graphite.[29] Thus, assuming an upward Fermi-level shift of 0.2 eV, excess electrons of about 0.004 per atom (an order of $10^{20}\,\mathrm{cm}^{-3}$) are necessary at the tip region in order to partly fill the conduction band. The defect density should be at least as large as this value. Now, we would like to estimate the size of the graphene sheet that gives such a defect density. For simplicity, we assume that a MWNT consists of small rhombic graphene sheets, each of which is similar to the unit cell of a graphene sheet. From a simple geometrical consideration, the numbers of carbon atoms in a rhombus and on the sides are $2l^2/a^2$ and $4l/a$, respectively, where $l(l \gg a)$ is

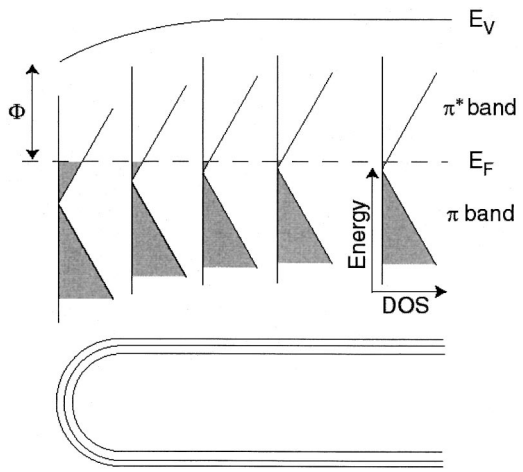

FIG. 9. Schematic energy diagram of a MWNT proposed in this study. E_v, E_F, and Φ denote the vacuum level, Fermi level, and the work function, respectively. The bands whose density of states (DOS) decreases and increases with the energy are the valence (π) band, and the conduction (π^*) band, respectively.

the side length of the rhombus and a the length of the unit vector of a graphene sheet (about 0.25 nm). It is expected that each carbon atom on the sides of the rhombus forms one defect state. Thus, the defect density in the rhombus becomes $2a/l$ on average. Therefore, l of ~120 nm gives a defect density of about 0.004 per atom. Our previous transmission electron microscopy (TEM) study[27] on deintercalated MWNT's revealed that most of the graphene sheets in the MWNT's had continuous lengths of only ~10 nm. If the length corresponds to the typical size of the graphene sheet in a MWNT, the defect density should be high enough to account for the observed Fermi-level shift.

Although our TEM observation revealed that both the tips and sidewalls of the MWNT's were intercalated,[26] it is likely that the defect density is larger at the spherically curved tips than at the cylindrically curved sidewalls. Therefore, we think that one possible explanation for the experimental results is that the Fermi level is pinned at a higher energy position at the tips than that at the sidewalls due to the larger defect densities at the tips as schematically shown in Fig. 9. The Fermi-level pinning will induce a redistribution of the electrons near the tip region to equalize the Fermi level along the tube axes, and the inner electric field induced by the electron redistribution causes band bending near the tips. This picture is similar to that observed at the GaAs(001) surface, where the Fermi level is pinned close to the midgap in spite of the doping type (n or p),[30] if the tube tips and sidewalls are replaced by the GaAs(001) surface and the bulk. It seems that, in contrast to MWNT's, SWNT's have much less defective structures, because intercalants in an intercalated SWNT bundle reside between the tubes in the bundle rather than inside the individual tubes if the SWNT's are capped.[12,31] Thus, the density of states at the Fermi level of the random MWNT's being larger than that of the SWNT's can be similarly explained by the larger defect density in MWNT's. That is, the Fermi level of the MWNT's is slightly shifted toward the conduction band from the ideal

position even at sidewalls, as also shown in Fig. 9.

Another possible explanation for the results on the aligned and the random MWNT's is that the defect density in the MWNT's strongly depends on the method of the synthesis. Namely, the MPE-CVD-grown aligned MWNT's are much more defective than the thermal CVD-grown random MWNT's. In any case, we would like to suggest that the defects play an important role in explaining the observed results. Although the electronic properties of carbon nanotubes have been discussed assuming ideal structures, they may be considerably affected by the defects, especially in MWNT's.

The experimental results obtained in this study have not been clearly obtained in previous STS studies. Other than the limited energy range of the scanning tunneling spectra, one of the possible reasons for this is that STS studies have focused mainly on SWNT's and thin MWNT's. Our previous study revealed that thinner MWNT's had more nearly perfect structures.[26]

V. CONCLUSIONS

The electronic structures of aligned and random MWNT's were investigated by photoemission spectroscopy. The spectra from the aligned and random MWNT's are considered to be dominated by photoemission from tube tips and sidewalls, respectively. A slight spectral shift to the higher-binding-energy side was observed both in the valence band and the C 1*s* spectra of the aligned MWNT's. The aligned MWNT's also showed a larger density of states at the Fermi level and a slightly smaller work function. All the results can be understood by assuming that the Fermi level is slightly shifted upward and located inside the conduction band at the tips of the aligned MWNT's. It seems to be difficult to explain the results assuming that the MWNT's have perfectly close-packed structures. We think that the Fermi level is pinned at the higher energy by the defect states at the tips of the aligned MWNT's. The electronic properties of MWNT's may be considerably affected by the defects.

ACKNOWLEDGMENTS

We thank Dr. T. Saitoh and Professor A. Kakizaki of Photon Factory, Institute for Material Structure Science, High Energy Accelerator Research Institute, Japan, for their support in this study. Work done at NTT was partly supported by Special Coordination Funds of the Science and Technology Agency of the Japanese Government. Work done at UNC was supported by the Office of Naval Research through a MURI program (N00014-98-1-0597).

*Corresponding author. Electronic address: ssuzuki@will.brl.ntt.co.jp

†Present address: NTT Telecommunications Energy Laboratories, Atsugi, Kanagawa, 243-0198 Japan.

‡Present address: Bell Laboratories, Lucent Technologies, Murray Hill, New Jersey 07974.

[1] W. A. de Heer, A. Chatelain, and D. Ugarte, Science **270**, 1179 (1995).

[2] Y. Saito, S. Uemura, and K. Hamaguchi, Jpn. J. Appl. Phys., Part 2 **37**, L346 (1998).

[3] W. Zhu, C. Bower, O. Zhou, G. Kochanski, and S. Jin, Appl. Phys. Lett. **75**, 873 (1999).

[4] R. Saito, M. Fujita, G. Dresselhaus, and M. S. Dresselhaus, Appl. Phys. Lett. **60**, 2204 (1993).

[5] J. W. G. Wildoer, L. C. Venema, A. G. Rinzler, R. E. Smalley, and C. Dekker, Nature (London) **391**, 59 (1998).

[6] D. L. Caroll, P. Redlich, P. M. Ajayan, J. C. Charlier, X. Blasé, A. D. Vita, and R. Car, Phys. Rev. Lett. **78**, 2811 (1997).

[7] P. Kim, T. W. Odom, J.-L. Huang, and C. M. Lieber, Phys. Rev. Lett. **82**, 1225 (1999).

[8] L. C. Venema, J. W. Janssen, M. R. Buitelaar, J. W. G. Wildoer, S. G. Lemay, L. P. Kouwenhoven, and C. Dekker, Phys. Rev. B **62**, 5238 (2000).

[9] C. Bower, W. Zhu, S. Jin, and O. Zhou, Appl. Phys. Lett. **77**, 830 (2000).

[10] R. Eisberg, G. Wiech, and R. Schlogl, Solid State Commun. **65**, 705 (1988).

[11] P. Chen, X. Wu, X. Sun, J. Lin, W. Ji, and K. L. Tan, Phys. Rev. Lett. **82**, 2548 (1999).

[12] C. Bower, S. Suzuki, K. Tanigaki, and O. Zhou, Appl. Phys. A: Mater. Sci. Process. **67**, 47 (1998).

[13] H. Ago, T. Kugler, F. Cacialli, W. R. Salaneck, M. S. P. Shaffer, A. H. Windle, and R. H. Friend, J. Phys. Chem. B **103**, 8116 (1999).

[14] R. Schlogl, Surf. Sci. **189/190**, 861 (1987).

[15] E. Frackowiak, S. Gaucher, S. Bonnamy, and F. Beguin, Carbon **37**, 61 (1999).

[16] G. K. Wertheim and P. H. Citrin, in *Photoemission in Solids I*, edited by M. Cardona and L. Ley (Springer, Berlin, 1978), pp. 197–236.

[17] S. Suzuki, C. Bower, Y. Watanabe, and O. Zhou, Appl. Phys. Lett. **76**, 4007 (2000).

[18] F. Maeda, T. Takahashi, H. Ohsawa, S. Suzuki, and H. Suematsu, Phys. Rev. B **37**, 4482 (1988).

[19] D. Marchand, C. Fretigny, M. Lagues, F. Batallan, Ch. Simon, I. Rosenman, and R. Pinchauxs, Phys. Rev. B **30**, 4788 (1984).

[20] C. Bower, O. Zhou, W. Zhu, A. G. Ramirez, G. P. Kochanski, and S. Jin, in *Amorphous and Nano-Structured Carbon*, edited by J. Robertson, J. Sullivan, O. Zhou, B. Coll, and T. Allen, Mater. Res. Soc. Symp. Proc. No. 593 (Materials Research Society, Pittsburgh, 2000), p. 215.

[21] S. Suzuki, C. Bower, T. Kiyokura, Krishna G. Nath, Y. Watanabe, and O. Zhou, J. Electron Spectrosc. Relat. Phenom. **114–116**, 225 (2001).

[22] S. H. Jhi, S. G. Louie, and M. L. Cohen, Phys. Rev. Lett. **85**, 1710 (2000).

[23] A. D. Vita, J.-Ch. Charlier, X. Blasé, and R. Car, Appl. Phys. A: Mater. Sci. Process. **68**, 283 (1999).

[24] M. Shiraishi and M. Ata, Carbon (to be published).

[25] Y. Miyamoto (unpublished).

[26] S. Suzuki and M. Tomita, J. Appl. Phys. **79**, 3739 (1996).

[27] O. Zhou, R. M. Fleming, D. W. Murphy, C. H. Chen, R. C. Haddon, A. P. Ramirez, and S. H. Glarum, Science **263**, 1744 (1994).

[28] S. Suzuki, Y. Watanabe, T. Kiyokura, K. G. Nath, T. Ogino, S. Heun, W. Zhu, C. Bower, and O. Zhou (unpublished).
[29] N. A. W. Holzwarth, in *Graphite Intercalation Compounds II*, edited by H. Zabel and S. A. Solin (Springer, Berlin, 1992), p. 18.
[30] M. D. Pashley and D. Li, J. Vac. Sci. Technol. A **12**, 1848 (1994).
[31] S. Suzuki, C. Bower, and O. Zhou, Chem. Phys. Lett. **285**, 230 (1998).